

Laser Behavior of (E, E)-2, 5-Bis [2-(1-Methyl-1H-Pyrrole-2-Yl) Pyrazine (BMPP) Dye Hybridized with CdS Quantum Dots (QDs) in Sol-Gel Matrix and Various Hosts

Mahmoud A. S. Sakr^{1,2}, Sayed A. Abdel Gawad², Samy A. El-Daly¹, Maram T. H. Abou Kana³ and El-Zeiny M. Ebeid^{1,2*}

¹Chemistry Department, Faculty of Science, Tanta University, Tanta, Egypt

²Misr University for Science and Technology (MUST), 6th of October City, Egypt

³National Institute of Laser Enhanced Sciences, Cairo University, Giza, Egypt

*Corresponding Author: Prof. Dr. El-Zeiny M. Ebeid, Department of chemistry, Faculty of science, Tanta University, Egypt, Email: elzeiny.ebeid@science.tanta.edu.eg

ABSTRACT

The present paper discusses the effect of CdS QDs on photo physical and photochemical parameters of BMPP laser dye in different media including methanol, sol-gel matrix, poly methyl methacrylate (PMMA) and a copolymer of MMA and 2-hydroxyethyl methacrylate (HEMA) media. CdS QDs have been applied as energy donors to BMPP laser dye in a trial to improve its lasing efficiencies and the sensitized emission of BMPP laser dye using CdS QDs as donors was also achieved in methanol.

The amplified spontaneous emission (ASE) efficiencies of BMPP laser dye in the different hosts under study were measured as the ratio between the output energy of the dye over a range of input pumping energy with a highest ASE slope efficiency being in methanol compared with PMMA and HEMA/MMA polymeric matrices.

The photo-stability of the samples was examined in terms of the ASE intensity change as a function of the exposure time to blue diode laser and in terms of the time needed to reduce the energy output intensity to half of its value. The highest photo stability was observed in methanol. The least stability is observed in PMMA and HEMA/MMA polymeric matrices. Despite the role of CdS QDs in sensitized emission, they enhance BMPP laser dye.

Some spectroscopic and photo physical criteria of BMPP dye have been measured in presence and absence of CdS QDs by applying spectroscopic data and relevant calculations. These include the oscillator strength, attenuation lengths, radiative decay rate constant, absorption and emission cross-sections, dipole moments, intersystem crossing rate constants and the tuning domain gain coefficients (α).

Keywords: Sol-gel, Quantum dots, Energy transfer and Photo stability

INTRODUCTION

The connection of nanoparticles (NPs) with fluorophores has been an active area of discussion during the last two periods with an enforcement ranging from material to biomedical science [1]. The fluorescence of a dye molecule is quenched or enhanced in the close nearness of NPs and can be utilized to test the microenvironment of the fluorophore.

The emission of a dye can be adjusted utilizing NPs and quenching or enhancement of photoluminescence of a dye by NPs dependent on the separation between dye molecule and NPs and mechanism of energy transfer [2]. There are of three kinds of quenching tasks:

static, dynamic and by electron / energy transfer. In static quenching, the dropping in emission intensity is a result of adsorption of the probe on the surface of QDs, activity a non-fluorescent complex among the fluorophore and quencher QDs, however, in dynamic quenching, the lowering of emission intensity is brought about by collision of the excited fluorophore with a quencher over the excited state lifetime. The third kind of quenching is because of radiative and non-radiative energy transfer among the dye molecule and QDs [3]. The fluorescence quenching is improved at shorter separations and it is relegated to proficient non-radiative energy transfer between a dye and the NPs [3].

The contradictions among radiative and non-radiative decay energy impacts the fluorescence of fluorophore molecules arranged close to the NPs because of Joule heating and surface Plasmon absorption in condition of metallic NPs. They have been utilized as gigantic and multilateral biological imaging specialists because of their high photo stability, high fluorescence quantum yields, large absorption coefficients, continual absorption bands for multi-color ability, narrow and symmetric emissions, and numerous bio- functionalization strategies which makes them perfect hopefuls as Forster resonance energy transfer (FRET) pairs[4,5].

In organic molecules, the high delocalized π -electron systems over their backbone have pulled in huge consideration due to potential applications related with strong emission attitude and gigantic nonlinear optical properties [6]. In Pyrazine [7] compound, the nitrogen atoms at the 1, 4 locations of a six membered aromatic ring. Because of the high electron withdrawing properties, pyrazines are brilliant choose for combination as electron-withdrawing groups in push-pull scaffolds supporting intra molecular charge transfer (ICT). Some distyryl pyrazines had been readied [8] and checked for optoelectronic gadgets, as emitting materials for lasing point [9]. In this article the spectral behavior of (E, E)-2, 5-bis [2-(1-methyl-1H-pyrrole-2-yl) pyrazine (BMPP) is examined in solution and in polymer network presence of CdS QDs.

Liquid dye lasers are high efficient, of low laser threshold, have wide tuning range from the near-UV to the near-IR regions of the spectrum and have long lifetime. None of other lasers can yet replace the dye laser for its power, gain, low price and broad range of tenability.

However, these lasers could not reach the commercial marketplace because of their inherent defects such as bulky volume, flammable and toxic solvents, dye degradation, heating and triplet-state formation.

Dye laser solutions have to be flowed through the laser cavity to maintain constant gain and beam quality. This requires bulky dye-flow systems and reservoirs, with large quantities of dye dissolved in often flammable and toxic solvents [10]. These hindrances can be conquering by doping stable laser dye molecules

into limited host network, for example, polymers, silica gels, xerogels and sol-gel glasses.

Inorganic glasses are excellent photonic media (in the spectral region of interest) because of their low optical losses, good mechanical properties (high strength, stiffness, hardness and introduction to hybrid organic-inorganic materials and abrasion resistance) and long-term environmental stability. In solid state dye lasers, dye-matrix interactions (hydrogen bonds between the dye and hydroxyls) allow the adsorption of the dye on the mesopores surface preventing the dye bimolecular reactions and enhance the dye thermal and environmental stability.

EXPERIMENTAL

Preparation of BMPP Dye-Doped Homopolymer Methyl Methacrylate (MMA)

MMA as homopolymer was prepared as follows: 3g/L of azobisisobutyronitrile (AIBN) as initiator was dissolved in purified MMA. The solution was placed in an ultrasonic bath for a period of about 15 min till the initiator was completely dissolved. Then BMPP dye was dissolved in MMA by using the ultrasonic bath for up to 20 min to obtain the desired concentration. Drying and aging were carried out in controlled clean oven at 60°C. After one week of preparation, the samples were dried and handled for various measurements [11].

Preparation of BMPP Dye- Doped Copolymer (MMA/ HEMA)

MMA/ HEMA copolymer was prepared as follows [12]: 3g/L of azobisisobutyronitrile (AIBN) as initiator was dissolved in freshly purified MMA and HEMA (1.5:1 ml) monomers. The solution was stirred in an ultrasonic bath for about 15 minute until the initiator was completely dissolved.

Then the BMPP dye was added to obtain the desired concentration and allowed to dissolve in the ultrasonic bath for extra 20 min. drying and aging were carried out in controlled clean oven at 60°C, since physical appearance and transparency were affected by increasing temperature over 60°C. After one week from the date of preparation, the samples got dried so they could be handled and subjected to various measurements.

Preparation of BMPP-Dye Doped Sol-Gel Matrix

Sol-gel materials were prepared by the hydrolysis of silicon alkoxide followed by poly condensation. fluorophore probe was doped into the matrix by doping method. Hydrochloric acid as a catalyst and glycerol as drying control chemical additives (DCCA) were added to get monoliths [10]. This method includes the additions of tetraethoxy silane (TEOS) 22.4 mL, methanol (MeOH) 12mL, distilled water (H₂O) 18mL, HCl 2mL (0.1N) and 16mL glycerol (Merck) as DCCA. The sol thus prepared was stirred in ultrasonic bath for 14.5 hours. Approximately one mL of laser dye methanolic solution and 2.5mL sol were poured into rectangular polystyrene cuvette and then sealed with Teflon tape. Drying and aging were completed in controlled clean oven at 60°C. After three weeks, the samples got dried so that it can be handled and can be subjected to various spectroscopic measurements [10].

Synthesis of Cadmium Sulphide Quantum Dots (CdS QDs)

Two methods for QDs preparation methods in both organic and aqueous media have been followed [13]. The QDs prepared in organic media gave frosty silicate samples upon doping whereas QDs prepared in aqueous medium gave clear appearance upon doping silicate hosts with QDs.

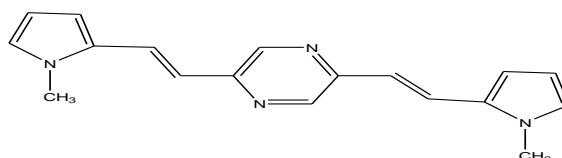
A typical procedure for the preparation of CdS QDs in organic medium was described as follows: 20.0mg cadmium acetate dihydrate [Cd(Ac)₂·2H₂O, 0.075 mmol] and 12.0mg sulfur powder (0.375 mmol) and 4mL oleic acid OLA were added into a 25mL three-neck flask [13]. Under nitrogen flow, the resulting solution was heated up to 250 °C and kept at this temperature for 4 h. The solution was then cooled to room temperature, and excess methanol was added to yield a yellow precipitate, which was then separated by centrifuging. After five times centrifugation and purification, CdS QDs were obtained and dissolved in toluene. All the solvents used were anhydrous and measurements were done at room temperature. Synthesized QDs were characterized by UV-Vis spectro photometer (PerkinElmer, Lambda 35) and fluorescence spectroscopy (PF-6300 Spectro fluorophotometer).

A typical procedure for the preparation of CdS QDs in aqueous medium was described as

follows [13]: 250 ml three-necked flask. 100 ml of 0.02M CdCl₂·2.5 H₂O was initially added in to the flask, then 1.0 ml thioglycolic acid was introduced under stirring, and the pH was adjusted to 12.00 using 1.0 M NaOH. After the solution was agitated for 10 min, 0.3ml of 30% H₂O₂ was added drop wisely into the flask. The reaction mixture was refluxed at 100°C under open air condition; an aliquot of sample was taken out at different times during the reflux. Absorption and transmission spectra of the prepared samples were recorded on a UV-Vis spectrophotometer (PerkinElmer, Lambda 35). The absorption spectral data of the dye-embedded with CdS QDs and undoped with CdS QDs were measured. The fluorescence spectra were recorded on assembled fluorometer (PF-6300 Spectro fluorophotometer) in front surface excitation-emission geometry. The excitation wavelengths were fixed at maximum absorption wavelengths (nm) for each fluorescence measurement.

Procedure of the Preparation of BMPP [12]

2, 5-dimethylpyrazine (0.00462 mol, 0.5 g) and 1-methylpyrrole-2-carboxaldehyde (0.0138 mol, 1.513 g) were dissolved in DMF and the mixture was cooled to 0°C. To this mixture, potassium-tert-but anolate (0.013 mol, 1.55 g) was added in small portions and the mixture was brought to ambient temperature and stirring was continued until all starting material had been consumed. After the completion of the response, water was included, and the product was isolated by extraction utilizing chloroform. The organic layer was concentrated in vacuum and the contained solid material acquired was recrystallized to give the product (1.2 g, 42%) as an orange solid. The structure of the compound was confirmed by IR and ¹H and ¹³C NMR spectroscopic techniques.



CHEMICAL STRUCTURE OF BMPP PROBE

Methods of Calculations

Portrayal of some photo physical properties of probe was performed hypothetically. The oscillator strength (*f*) values were determined from equation (1) [12, 13].

$$f = 4.32 \times 10^{-9} \int \epsilon(\tilde{\nu}) d\tilde{\nu}, \quad (1)$$

Where $\tilde{\nu}$ is the wave number and ϵ is the molar extinction coefficient. Scientifically, The estimation of (f) is subject to the sub-atomic structure. The attenuation length $\Lambda(\lambda)$ (the separation at which the original light intensity I_0 is diminished to $I = I_0/e$, is given by equation (2) [14].

$$\Lambda(\lambda) = \frac{1}{\epsilon(\lambda)c \ln(10)}, \quad (2)$$

Where $\epsilon(\lambda)$ is the molar extinction coefficient and c is the molar concentration. The Λ values are essentially reliant on the wavelength. The change dipole moment μ_{12} from ground to excited state was determined by utilizing equation (3) [15].

$$\mu_{12}^2 = \frac{f}{4.72 \times 10^{-7} E_{\max}}, \quad (3)$$

Where E_{\max} is the maximum energy of absorption in cm^{-1} .

The radiative decay rate constant (k_r) of a fluorophore can be hypothetically anticipated from the notable Strickler-Berg equation, which has its establishments on Einstein's spontaneous emission rate and Planck's black body radiation law equation (4) [16, 17].

$$k_r = \frac{1}{\tau_0} = 2.88 \times 10^{-9} n^2 \frac{\int F(\tilde{\nu}) d\nu}{\int F(\tilde{\nu}) \tilde{\nu}^{-3} d\nu} \int \frac{\epsilon(\tilde{\nu})}{\tilde{\nu}} d\tilde{\nu}, \quad (4)$$

Where $F(\tilde{\nu})$ is the fluorescence intensity, $\tilde{\nu}$ is the wave number and $\epsilon(\tilde{\nu})$ is the molar extinction coefficient at a particular wave number ($\tilde{\nu}$), n is the refractive index of the solid host. The absorption cross-section σ_a is given by equation (5) [18].

$$\sigma_a = 0.385 \times 10^{-20} \epsilon(\lambda). \quad (5)$$

The fluorescence intensity of the dye- embedded solid was normalized. To determine the quantum yield of a compound relative to a standard probe, the following relationship (6) was applied [19].

$$\phi_u = \phi_s \times \frac{I_u}{I_s} \times \frac{A_s}{A_u} \times \frac{n_s^2}{n_u^2}. \quad (6)$$

Where ϕ_u and ϕ_s are the fluorescence quantum yields of the unknown and the standard respectively. I_u And I_s are the areas under emission curves for the unknown and the standard respectively.

A_u And A_s are the absorbance of the unknown, and the standard respectively. n_s and n_r are the refractive indices of solvents used.

Fluorescence lifetimes (τ_f) were calculated by using equation (7).

$$\tau_f = \tau_0 \phi_f, \quad (7)$$

Where (τ_0) is the natural lifetime ($\tau_0 = 1/k_r$). The intersystem crossing rate constant (k_{isc}) is identified with the quantum fluorescence yield ϕ_f for ($\phi_f \approx 1$) the rough relationship (8) [20]:

$$k_{isc} = (1 - \phi_f) / \tau_f, \quad (8)$$

Where ϕ_f is the fluorescence quantum yield.

The emission cross-section σ_e was determined according to equation (10) [16].

$$\sigma_e = \frac{\lambda^4 F(\lambda) \phi_f}{8\pi c n^2 \tau_f}, \quad (10)$$

Where λ is the emission wavelength, n the refractive index of the host, ϵ is the extinction coefficient, c the velocity of light, $F(\lambda)$ is the normalized fluorescence spectrum where $\int F(\lambda) d\lambda = 1$ and ϕ_f is the fluorescence quantum yield.

BMPP probe in various media were pumped by Diode continuous laser ($\lambda_{ex} = 450$ nm) of 160mW energy. The greatest gain coefficient (α) was determined at the most extreme laser emission by estimating the intensity I_L of laser emission from the whole cell length L and the intensity $I_{L/2}$ from the cell half-length. The beam gain was then assessed from equation (11) [21].

$$\alpha(\lambda) = \frac{2}{L} \ln \left[\frac{I_L}{I_{L/2}} - 1 \right]. \quad (11)$$

In light quantum mechanical bother hypothesis, the absorption and fluorescence band shift of a spherical is described by equations [22].

$$\nu_a - \nu_f = m_1 f(\epsilon, n) + const. \quad (12)$$

$$\nu_a + \nu_f = -m_2 [f(\epsilon, n) + 2g(n)] + const. \quad (13)$$

Where ν_a and ν_f are the absorption and fluorescence frequencies peaks, and

$$f(\epsilon, n) = \frac{2n^2 + 1}{n^2 + 2} \left[\frac{\epsilon - 1}{\epsilon + 2} - \frac{n^2 + 1}{n^2 + 2} \right] \quad (14)$$

Is the solvent polarity parameter [23] and,

$$g(n) = \frac{3}{2} \left[\frac{n^4 - 1}{(n^2 + 2)^2} \right] \quad (15)$$

With

$$m_1 = \frac{2(\mu_e - \mu_g)^2}{hca^3} \quad (16)$$

And

$$m_2 = \frac{2(\mu_e + \mu_g)^2}{hca^3} \quad (17)$$

Where h is Plank's constant, c is the velocity of light in vacuum and a is Onsager cavity radius of the probe molecule where as μ_g and μ_e are the ground and excited state dipole moments respectively. The parameters m_1 and m_2 can be determined from equation (12) and (13). Upon rearrangement of equations (16) and (17), the values of μ_g and μ_e can be determined from equations (18) and (19) assuming that the symmetry of the probe molecule remains unchanged upon electronic transition, and the ground and excited state dipole moments are parallel [24],

$$\mu_g = \frac{|m_2 - m_1|}{2} \left[\frac{hca^3}{2m_1} \right]^{\frac{1}{2}} \quad (18)$$

$$\mu_e = \frac{|m_2 + m_1|}{2} \left[\frac{hca^3}{2m_1} \right]^{\frac{1}{2}} \quad (19)$$

$$\frac{\mu_e}{\mu_g} = \frac{|m_2 + m_1|}{|m_2 - m_1|} \quad (20)$$

Parameters m_1 and m_2 are linear functions of the solvent polarity parameters f (ϵ , n) and f (ϵ , n) + 2g (n) and can be determined from the slopes of straight lines. Also, the Onsager cavity radius a can be determined by computational calculations.

The change in dipole moment ($\Delta\mu$) between the excited singlet and ground state has been researched utilizing the solvate chromic shift by Reichardt [25]. In this method, change in dipole moment is calculated by correlating the Stokes shift of the fluorophore to E_T^N according to equation (21) [26, 27]

$$\nu_a - \nu_b = 11307.6 \left[\left(\frac{\Delta\mu}{\Delta\mu_B} \right)^2 \left(\frac{a_B}{a} \right)^3 \right] E_T^N + const. \quad (21)$$

where $\Delta\mu$ is the difference between the excited and ground state dipole moments of the probe molecule and $\Delta\mu_B$ (taken as 9 Debye) is the change in the dipole moment of the betaine dye; a and a_B are the Onsager cavity radius of the probe molecule and betaine molecule, respectively. The values of a and a_B are known (4.34 Å and 6.2 Å respectively).

Water and tetra methyl silane (TMS) as reference solvents are used to determine the solvent polarity E_T^N according to the following equation

$$E_T^N = \frac{E_T(\text{solvent}) - E_T(\text{TMS})}{E_T(\text{water}) - E_T(\text{TMS})} = \frac{E_T(\text{solvent}) - 30.7}{32.4}$$

$$ET = 28591 / \lambda_{\max} \text{ (nm)} \quad (22)$$

Where λ_{\max} corresponds to the peak wave length in the red region of the intra molecular charge transfer absorption of the probe. Then the change in dipole moment is

$$\Delta\mu = \mu_e - \mu_g = \sqrt{\frac{m \times 81}{\left(\frac{6.2}{a}\right)^3 \times 11307.6}} \quad (23)$$

Here m is the slope of linear plot of E_T^N against Stokes shift. The sizes of CdS QDs were controlled by equation [10] (24):

$$D = (1.6122 \times 10^{-9})\lambda^4 - (2.6575 \times 10^{-6})\lambda^3 + (1.6242 \times 10^{-3})\lambda^2 - (0.4277)\lambda + (41.57) \quad (24)$$

$$\epsilon = 5857(D)^{2.65} \quad (25)$$

D (nm) is the size of a given QDs sample = 2nm, λ (nm) is the wavelength and ϵ is the molar absorptive of the first excitonic absorption peak of the corresponding sample.

RESULTS AND DISCUSSION

Upon using equation (25), the molar concentration of CdS QDs was calculated as 6.6×10^{-6} mol/L [10]. The size of CdS QDs has been determined hypothetically as 3-5nm. The canary yellow CdS QDs were described by UV-Vis absorption spectro photometry and transmission electron microscope (TEM). CdS QDs display maximum absorption at 411 nm and a maximum emission at 450nm. BMPP laser dye methanolic solutions show a maximum absorption at 449 nm and a maximum emission at 549 nm. Figure 1 demonstrates the overlap

Laser Behavior of (E, E)-2, 5-Bis [2-(1-Methyl-1H-Pyrrole-2-Yl)] Pyrazine (BMPP) Dye Hybridized with CdS Quantum Dots (QDs) in Sol-Gel Matrix and Various Hosts

between BMPP dye UV-Vis absorption and CdS QDs fluorescence spectra. The absorption and fluorescence spectra of ($1 \times 10^{-5} \text{M}$) BMPP dye were recorded in solvents of different polarities and in various confined hosts (MMA homopolymer, (HEMA/MMA) copolymer and silica matrix) with and without CdS QDs. Sol-gel network demonstrates the benefit of being transparent in the UV region down to 250 nm where as PMMA and HEMA/MMA are most certainly not.

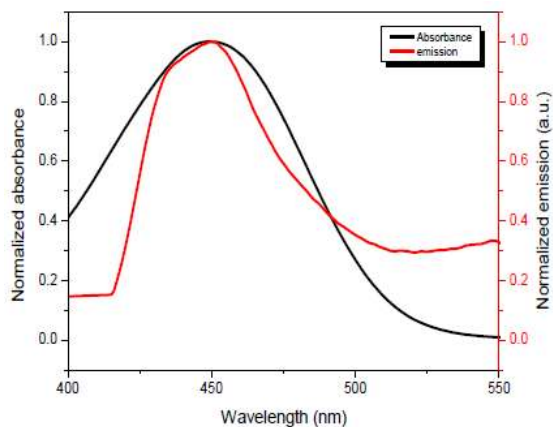


Figure1. The spectral overlap of $1 \times 10^{-5} \text{M}$ BMPP dye absorption and $6.6 \times 10^{-6} \text{mol/L}$ CdS QDs emission ($\lambda_{ex} = \text{Nm}$) spectra in methanol.

Because sol-gel silicate matrix was prepared by acid catalysis, it was necessary to study the acid-base behavior of BMPP laser dye that possesses lone pair electrons on four nitrogen atoms. Referring to BMPP structure, the two pyrrole ring nitrogens are expected to be more basic (being of sp^3 hybridization) than the two pyrazine nitrogens (being of sp^2 hybridization). Figure 2-shows the electronic absorption spectra of $1 \times 10^{-5} \text{M}$ BMPP dye in neutral and acidified methanolic solutions. Two distinct behaviors are observed, one at pH values higher than 4 in which the pyrrole nitrogens are protonated giving a short wavelength peak appears at a 322 nm at the expense of the long wavelength band at 449 nm.

At pH values lower than pH 4, protonation of less basic pyrazine nitrogens occurs giving highly ionic species that become sparingly soluble in methanol organic solvent and the absorption bands virtually disappear. In aqueous buffers, the short wavelength peak are observed down to $\text{pH} = 1$ value.

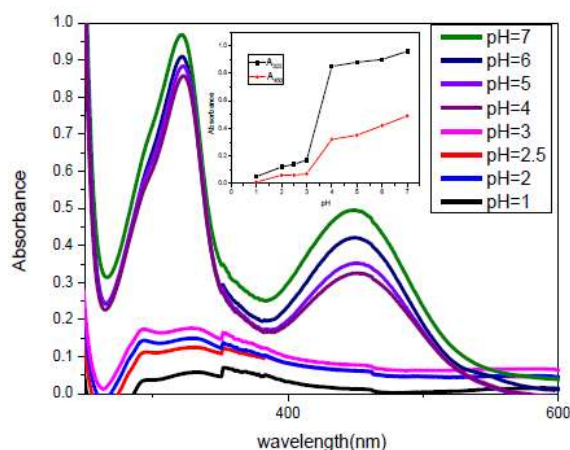


Figure2a. Electronic absorption spectra of $1 \times 10^{-5} \text{M}$ BMPP dye in methanol at different pH values. The inset shows the plot of absorbance versus pH.

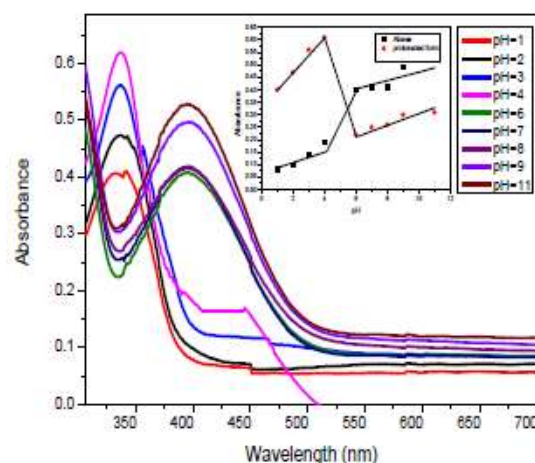


Figure2b. Electronic absorption spectra of BMPP ($1 \times 10^{-5} \text{mol L}^{-1}$) at different pH values. The inset shows the plot of absorbance versus pH.

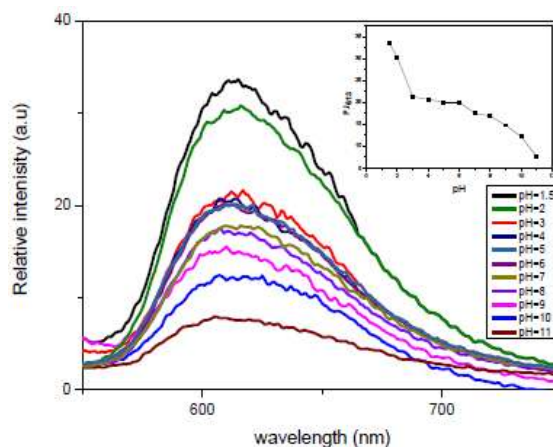


Figure2c. Emission spectra of BMPP ($1 \times 10^{-5} \text{mol L}^{-1}$) at different pH values. The inset shows the plot of emission intensity versus pH

The impact of medium acidity on the electronic absorption and emission spectra of BMPP have been examined in aqueous buffers covering the pH range from 1.5 to 11 as shown in Figures (2-

b and 2-c). The absorption maximum is moved from 395 to 337 nm (blue-shift) as shown in Fig.2-b because of protonation of pyrrole ring nitrogen atom in BMPP dye [28]. The fluorescence intensity decreased sharply upon decreasing the acidity of medium without any shift in the wavelength of the emission band, due to the formation of the non-emissive protonated form [28] (Fig.2-c). The ground-state protonation constant (pK_a) was determined from the absorbance changes at 395 and 337 nm, in addition to from the variation of λ_{max} with pH. The protonation constant of the excited state (pK_a^*) was determined using spectro photometric titration and Forster's cycle using the following relation $pK_a - pK_a^* = 2.1 \times 10^{-3}(\nu_{BH^+} - \nu_B)$, [28] where $(\nu_{BH^+} - \nu_B)$ represents the difference between the wave number (cm-1) of electronic transition of pure acidic and conjugate base, respectively. The estimations of pK_a were resolved as 5.16 and 5.96 from absorption and emission spectra, respectively, with an average pK_a as 5.56.

The pK_a^* value calculated from the absorption spectral shift is calculated as -3.58, indicating that the singlet excited state of BMPP is more acidic than the ground state [28]. Sensitized emission of BMPP dye utilizing CdS QDs as donor is shown in Figure 3 in methanol demonstrating energy transfer from CdS QDs (donors) to this probe dye (acceptor).

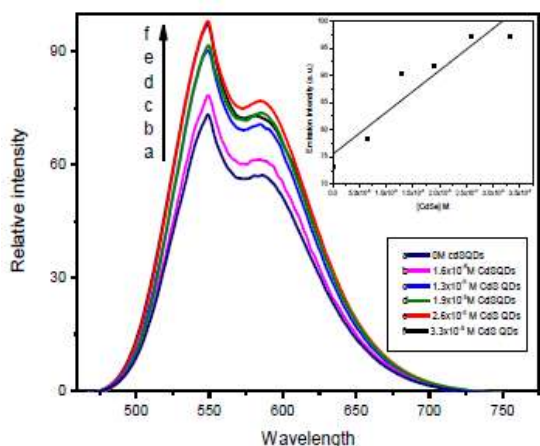


Figure3. Sensitized emission of $1 \times 10^{-5} M$ of BMPP laser dye in methanol (top; $\lambda_{ex.} = 411 \text{ nm}$) using different concentrations of CdS QDs as donor. The inset shows emission intensity of BMPP probe at different concentration CdS QDs.

The ASE efficiencies of BMPP laser dye in the different hosts under investigation were estimation as the ratio between the output energy of the dye over a range of input pumping energy. It has been examined and represented in Fig.4. The samples were transversely pumped and were allowed to emit in the highest peak intensity of the mirror less ASE (a.u.). The pump energy was controlled and varied between 160 to 300 mW. In general, the output energy increased with increasing the pumping energy for all samples with a highest ASE slope efficiency in methanol compared with PMMA and HEMA/MMA polymeric matrices.

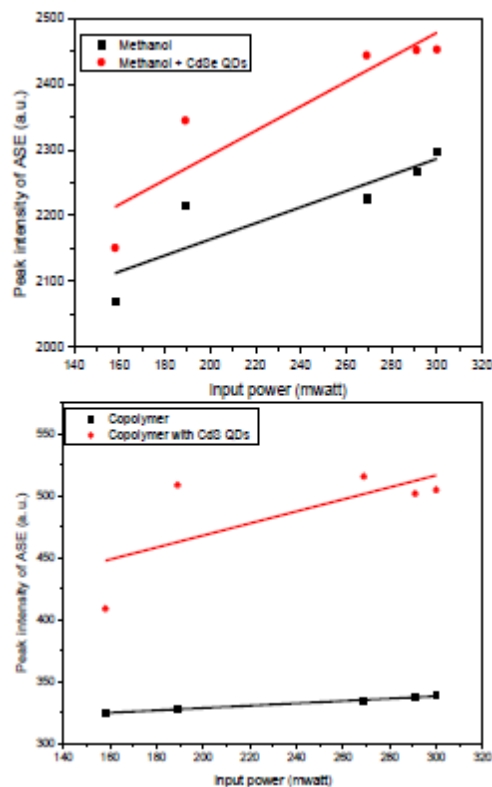


Figure4. ASE output intensity of $1 \times 10^{-3} M$ BMPP (without and with $1.6 \times 10^{-6} M$ CdS QDs) as a function of input energy in methanol (top) and in copolymer medium (bottom).

The photo-stability of the samples was examined in terms of the ASE intensity change as a function of the exposure time to blue diode laser of 450 MW as shown in Fig.5. The highest photo stability is observed both in methanol. The least stability is observed in PMMA and HEMA/MMA polymeric matrices. This may be attributed to the presence of carbonyl group in PMMA and HEMA/MMA polymeric matrices the enhances intersystem crossing (k_{isc}) leading to triplet state population.

Laser Behavior of (E, E)-2, 5-Bis [2-(1-Methyl-1H-Pyrrole-2-Yl)] Pyrazine (BMPP) Dye Hybridized with Cds Quantum Dots (QDs) in Sol-Gel Matrix and Various Hosts

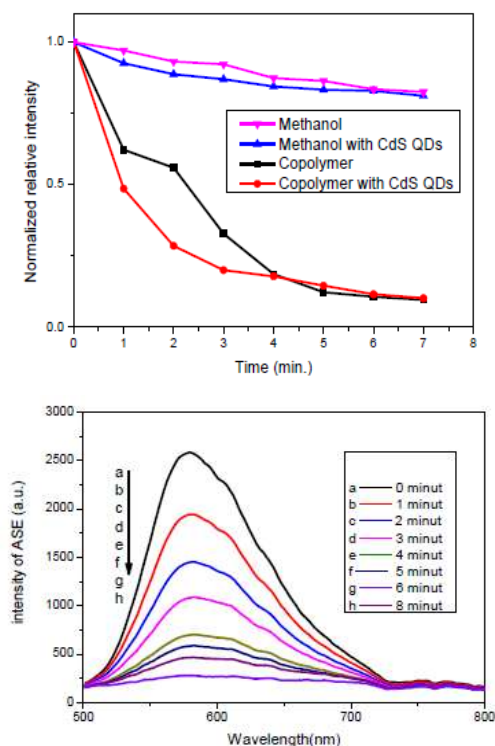


Figure5. ASE output energy as a function of exposure time for BMPP laser dye in different hosts using diode continuous laser ($\lambda=450$ nm) (top) and in methanol (bottom).

The photo-stability of the samples was also examined in terms of the time needed to reduce the energy output intensity to half of its value for BMPP laser dye concentration $1 \times 10^{-3} M$ without and with CdS QDs. Table.4 lists the lasing range, the maximum wavelength of mirror less amplified spontaneous spectra (ASE), and the half life time at which a 50% reduction in the intensity of the material occurs. The half-life time of BMPP laser dye in methanol, and copolymer is 50 min and 2.23 min in absence CdS QDs respectively. So, the half-life time of BMPP probe dye is higher in methanol compared with polymeric matrices. Fig. 6 shows the ASE output energy of

fluorescein as a function of exposure time under the same conditions for comparison.

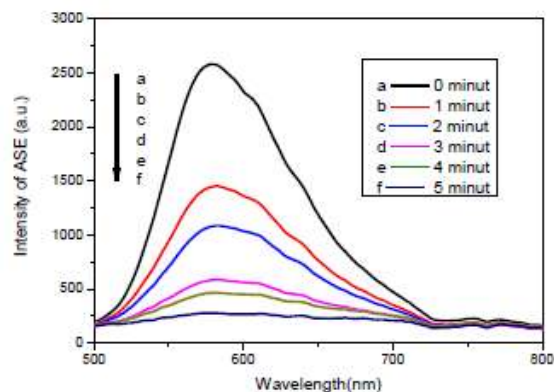


Figure6. ASE output energy as a function of exposure time for $1 \times 10^{-3} M$ BMPP laser dye in methanol in presence of $1.6 \times 10^{-6} M$ CdS QDs using diode continuous laser ($\lambda=450$ nm).

Some photo-physical criteria of BMPP dye have been measured in presence and absence of CdS QDs by applying spectroscopic data and equations 1-10. Upon adding CdS QDs, the oscillator strength values of electronic transitions of BMPP laser dye increase in organic solvents but decrease in solid hosts. Because the dynamic interaction between QDs and dye molecules in solvents is higher than in solid hosts. Also, the oscillator strength values of BMPP dye in sol-gel matrix are higher than those in copolymer and homo polymer matrix. This is because the mobility of dye molecules in sol-gel is higher than in copolymer. Hence, the effective number of electrons transferred from the ground to excited states in sol-gel is higher than in copolymer and homo polymer matrices. For BMPP laser, the attenuation length values of the probe in free solvents are higher than those in restricted hosts. Addition of CdS QDs affects the attenuation lengths values as shown in Table 1.

Table1. Spectral and photo physical data of BMPP in different solvents and restricted hosts (with and without CdS QDs).

Hosts	$\lambda_{abs.}(nm)$		$\epsilon M^{-1}cm^{-1}$		f		$\lambda_{(cm)}$		$k_r \times 10^9 s^{-1}$		$\sigma_a \times 10^{(-16)} cm^2$		$\mu_{12}(D)$	
	Without QDs	With QDs	Without QDs	With QDs	Without QDs	With QDs	Without QDs	With QDs	Without QDs	With QDs	Without QDs	With QDs	Without QDs	With QDs
Methanol	449	448	50000	58000	0.93	0.94	0.86	0.74	2.24	2.66	1.93	2.23	9.41	9.45
2-propanol	451	449	17300	17300	0.69	0.83	2.51	2.51	4.43	1.65	0.66	0.66	8.12	8.906
Hexane	442	441	25300	25300	0.95	0.96	1.71	1.71	7.89	3.23	0.99	0.97	10.87	10.89
Dioxane	446	448	29200	29200	0.77	1.06	1.48	1.48	3.72	4.07	1.12	1.12	8.568	10.05
chloroform	445	451	30200	30200	0.97	0.98	1.43	1.43	5.34	5.35	1.16	1.16	9.649	9.699
Acetonitrile	440	440	25800	25800	0.89	0.90	1.68	1.68	2.62	3.32	1.68	0.99	9.129	9.18
PMMA	368	368	76000	56700	0.80	0.51	0.57	0.98	4.80	1.31	2.92	1.69	9.125	7.455
Copolymer	337	337	67000	67000	0.95	0.80	0.64	0.64	1.17	0.75	2.57	2.57	10.13	9.30
Sol-gel	300	300	82000	77000	0.96	0.85	0.52	0.56	4.47	0.41	2.23	3.15	7.81	7.35

Laser Behavior of (E, E)-2, 5-Bis [2-(1-Methyl-1H-Pyrrole-2-Yl) Pyrazine (BMPP) Dye Hybridized with CdS Quantum Dots (QDs) in Sol-Gel Matrix and Various Hosts

Radiative decay rate constant (k_r) values have also been calculated for BMPP and [BMPP / CdS QDs] in free solvents and contrasted to values in restricted media. The calculated values are given in Table 1. In presence of CdS QDs, k_r values of BMPP emission are lower in restricted matrices compared with methanol, dioxane, chloroform and acetonitrile. This implies longer natural lifetime (τ_0) values in restricted matrices as a result of imposed cage effect. Both absorption and emission cross-sections were calculated for the BMPP dye in restricted media and different solvents (Tables 1 and 2). Upon adding CdS QDs, the absorption cross sections (σ_a) of BMPP in hexane, acetonitrile and PMMA decrease. However, the values of σ_a are

not influenced in 2-propanol, hexane, chloroform and copolymer. But the values of σ_a increase in methanol and in sol-gel matrix as shown in Table 1. The values of absorption and emission cross sections agree with values reported for other efficient laser dyes [18]. In different solvents, the k_{isc} values of [BMPP/CdS QDs] increase. But in restricted media, the values of k_{isc} of [BMPP/CdS QDs] are lower than those of BMPP dye alone. This is an important criterion since it implies less triplet population in the [BMPP/CdS QDs] system in restricted media making it better lasing system. Singlet-triplet splitting energies ($\Delta E_{S,T}$) are decreased in solvents but it is increased in restricted media.

Table2. Spectral and photo physical data of BMPP in different solvents and restricted hosts (with and without CdS QDs).

Hosts	λ_f (nm)		τ_f (ns)		$\sigma_e \times 10^{-17} \text{ cm}^2$		E_f		$k_{isc} \times 10^9 \text{ s}^{-1}$	
	Without QDs	With QDs	Without QDs	With QDs	Without QDs	With QDs	Without QDs	With QDs	Without QDs	With QDs
Methanol	549	548	0.17	0.07	1.90	1.97	0.16	0.16	3.50	10.60
2-propanol	546	545	0.06	0.06	1.15	1.08	0.08	0.05	11.50	12.30
Hexane	540	539	0.24	0.24	2.68	2.07	0.41	0.05	2.07	2.58
Dioxane	546	546	0.07	0.07	4.05	2.51	0.08	0.06	10.3	12.00
Chlorofom	533	545	0.05	0.06	2.94	2.95	0.17	0.05	8.51	11.80
Acetonitrie	530	533	0.06	0.19	2.25	2.06	0.05	0.07	11.8	3.93
PMMA	489	512	0.19	0.28	1.82	0.55	0.0065	0.0069	3.92	2.82
Copolymer	508	508	0.10	0.10	0.48	0.28	0.0013	0.0092	7.13	7.12
Sol-gel	357	357	0.05	0.53	1.67	1.20	0.04	0.18	12.5	1.47

Table 1 shows the calculated transition dipole moments (μ_{12}) that possess higher values in methanol, chloroform, 2-propanol and hexane and dioxane but lower values in both PMMA and copolymer matrices in presence of CdS QDs. This indicates that CdS QDs increase intra molecular charge transfer in free solvents compared to solid matrices. The molecular polarity depends on its electron distribution. The absorption of an additional energy will cause the transition of an electron from HOMO to LUMO orbitals. This will cause variation in dipole moment with respect to the ground state dipole moment [29]. The emission spectra have been recorded by exciting the sample at its absorption

maximum. The shift in the absorption and emission maxima has been plotted as a function of solvent polarity. In order to estimate the ground and excited state dipole moments of the BMPP dye molecule, the solvent polarity parameters $f(\epsilon, n)$ and $f(\epsilon, n) + 2g(n)$ were calculated. The respective spectral shifts $\nu_a - \nu_f$ and $\nu_a + \nu_f$ for the BMPP dye with and without CdS QDs were plotted versus the polarity function $f(\epsilon, n)$ and $f(\epsilon, n) + 2g(n)$ respectively. The plots show a linear correlation. The slopes m_1 and m_2 of the paired plots were used to estimate the ground and excited state dipole moments listed in Table 3.

Table3. Dipole moments, slope (m) of BMPP laser dye by Biolt method.

Compound	$m_1(\text{cm}^{-1})$	$m_2(\text{cm}^{-1})$	$g^{-1}\mu_e\mu$	$g(\text{D})\mu$	$e(\text{D})\mu$	
BMPP	With CdS QDs	633	1738	2.21	1.89	4.05
	Without CdS QDs	25	538	0.43	4.41	4.84

Table 3 shows that the excited state dipole moment is larger than ground state one indicating that a large intra molecular charge transfer is taking place in the excited state in

comparison to the ground state, confirming the presence of $\pi-\pi^*$ transition in BMPP dye. Table 3 also shows that the ground and excited state dipole moments decreased in present of CdS

QDs as the lone pair electrons of sp^3 hybridized ring nitrogen atoms cannot make coordination bond with CdS QDs presumably due to steric hindrance. Solvato chromic shift method was acquainted by Reichardt [30] with research the change in dipole moment ($\Delta\mu$) between excited singlet and ground states relying up on microscopic solvent polarity parameter E_T^N given by the Eq. (22). The principle preferred stand point of this method over the Lippert–Mataga method is the incorporation of hydrogen bonding in addition to the solvent polarity into the solvent parameters. In this method, change

in dipole moment is calculated by correlating the Stokes shift of the fluorophore probe to E_T^N according to Eq. (21) in which “a” was taken as 4.34 for the dye. The dipole moment change was calculated according to eq. (23) where the slopes of linear plots of E_T^N vs stokes shift (m) equal 7199.65cm^{-1} and 7306cm^{-1} in presence and absence of CdS QDs respectively. The estimations of $\Delta\mu$ were observed to be 4.20 and 4.23D in the presence and absence of CdS QDs respectively. The high value of $\Delta\mu$ proposes that the singlet excited state of BMPP is of strong intermolecular charge transfer (ICT) character.

Table4. Mirror less laser parameters of BMPP in methanol and copolymer medium

Host	Lasing range		$\lambda_{\text{max}}(\text{nm})$		$\alpha (\text{cm}^{-1})$	
	Without QDs	With QDs	Without QDs	With QDs	Without QDs	With QDs
Methanol	538-556	529-571	549	548	0.29	0.41
Copolymer	471-538	471-538	510	501	3.35	2.27

The steady state absorption and emission data in a range of various solvents are given to quantify solvent polarities. The empirical π^* scales propounded by Kamlet et al [31] were utilized. The empirical parameters π^* , α and β which, respectively, measure the solvent dipolarity/polarizability, hydrogen-bond donor acidity, and hydrogen-bond acceptor basicity. The Taft and Kamlet equation relates these parameters to the absorption or emission data, expressed in wave

number (ν). It tends to be composed as [32] ($\nu = \nu + s\pi^* + \alpha\alpha + b\beta$) where; s, a and b are the coefficients for the π^* , α and β parameters respectively. Information about the different solute/solvent interactions can be obtained by monitoring the solvent-induced spectral shifts, the effect of solvents (with and without CdS QDs) on the absorption and emission wave numbers (ν_a and ν_e in cm^{-1} , respectively). The following multiple regressions were applied:

Without CdS QDs	$\nu_a=18288+391\pi^*-301\alpha-687\beta$, $\nu_e=22458-19\pi^*-381\alpha-489\beta$
With CdS QDs	$\nu_a=18442-24\pi^*-233\alpha-283\beta$, $\nu_e=22586-318\pi^*-260\alpha-183\beta$

Incorporation of the π^* parameter was necessary to improve the correlation coefficient especially in the case of ν_e . Accordingly, the shift of the absorption band was monitored mainly by the dipolar and hydrogen bond donating interactions with the solvent molecules while the solvent basicity contributes to the shift of the fluorescence maximum. Upon adding CdS QDs, the coefficients of α and β in ground and excited states decreased. In the ground state, the coefficients of π^* decrease. The larger value of the coefficient representing contribution of the dipolar interaction in the excited state (relative to the ground state) indicates enhanced charge separation upon excitation.

CONCLUSION

Photo-physical parameters and ASE optical performance of BMPP dye in liquid and solid hosts were studied. As shown from ASE spectra, CdS QDs increase the photo degradation of

BMPP dye in methanol and copolymer. Highest ASE slope efficiency being in methanol compared with PMMA and HEMA/MMA polymeric matrices. The highest photo stability was observed both in methanol compared with PMMA and HEMA/MMA polymeric matrices. The photo physical properties were investigated in organic solvents. It is inferred from the absorption and emission spectra that emissive state of BMPP has intermolecular charge transfer characteristics.

The incorporation of BMPP laser dye in copolymer was prepared successfully. The fluorescence quantum yield depends on the polarity of solvent as well as specific solute/solvent interaction such as hydrogen bond CdS QDs is decreased coefficients of α and β in ground and excited state, but coefficient of π^* is decreased in ground state and increased in excited state.

REFERENCES

- [1] Wei D. and Goldys E.M. Plasmonic approach to enhanced fluorescence for applications in biotechnology and the life sciences. *J. Langmuir* 28, 10152–10163, (2012).
- [2] Suchita k., Aparna C. D. and Shashi B. S. Tuning luminescence intensity of RHO6G dye using silver nanoparticles. *J. Bull. Mater. Sci.* 31, 541–544, (2008).
- [3] Pushpam S., Kottaisamy M. and Ramakrishnan V., Dynamic quenching study of 2-amino-3-bromo-1, 4-naphthoquinone by titanium dioxide nano particles in solution (methanol) *J. SpectrochimActa* 114, 272–276, (2013).
- [4] Talapin D.V., Rogach A. L., Mekis I., Haubold S., Kornowski A., Haase M. and Weller H., synthesis and surface modification of amino-stabilized CdSe, CdTe and InP nanocrystals. *J. Colloids Surf. A* 202, 145-154 (2002).
- [5] Aliaksandra R., Diana S., Tatsiana R., John F. D., Yury P.R., Vincent K., Vladimir L. and Alexander E., CdTe Quantum Dot/Dye Hybrid System as Photosensitizer for Photodynamic Therapy *J. Nanoscale Res Lett* 5, 753–760 (2010).
- [6] Kim H. N., Guo Z., Zhu W., Yoon J. and Tian H. Recent progress on polymer-based fluorescent and colorimetric chemosensors, *J. Chem. Soc Rev* 40, 79–93, (2011).
- [7] Castle R. N. Chemistry of heterocyclic compounds, John Wiley and Sons, New York, 23 (1962).
- [8] Scaccianocce L., Feeder N., Teat S. J., Marseglia E. A, Grimsdale A. G. and Holmes A. B. A synchrotron diffraction study of two polymorphic forms of 2,5-bis[2-(4 methoxy phenyl) ethenyl] pyrazine, *J. ActaCrystallogr C* 56, 1277–1279 (2000).
- [9] Al- Hazmy S. M., Babaqi A. S, Daltrozzo E., Klink M., Sauter J. and Ebeid E. M. A new diolefinic laser dye: 2, 5-bis-2-(2-naphthyl) vinyl pyrazine (B₂NVP) *J. PhotochemPhotobiol a Chem* 122, 17–22 (1999)
- [10] Deshpande A. V. and Kumar U., Effect of method of preparation on photophysical properties of Rh-B impregnated sol–gel hosts *J. Non-Cryst.Solids*.306, 149 -159 (2002).
- [11] Sakr M. A. S., Abdel Gawad E. A., Abou Kana M. T. H. and Ebeid E. M. Photo physical, photochemical and laser behavior of some diolefinic laser dyes in sol-gel and methyl methacrylate/2-hydroxyethyl methacrylate copolymer matrices. *J. Opt Laser Technol* 71, 78-84 (2015).
- [12] El-Daly S. A., Abdullah M. A., Khalid A. A. and Osman I. O., A ratio metric rhodamine–naphthalimide pH selective probe built on the basis of a PAMAM light-harvesting architecture. *J. photochemistry and photobiology A*, 312, 64-72 (2015).
- [13] Bojinov V. And Grabchev I. Synthesis and photo physical investigations of novel combined benzo [de]anthracen-7-one/2, 2, 6, 6-tetramethyl piperidines as fluorescent stabilizers for polymer materials. *Polymer degradation and Stability*. 85, 789 -797(2004); Wang Y., Lu J., Tong Z., Li B. and Zhou L. facile synthesis of CdS nanocrystals using thioglycolic acid as a sulfur source and stabilizer in aqueous solution. *J. Bull. Chem. Soc. Ethiop.* 25, 393-398 (2011).
- [14] Elisei F., Gattib F., Goretti C. A., Hagnerd T., Masetti F., Mazzucato U., Ranucci G., Schoenertd S., Testerab G., Ullucci P. and Vitaleb S. Measurements of liquid scintillator properties for the Borexino detector *J. NuclInstrum Meth Phys Res a* 400, 53-68 (1997).
- [15] Briks J. B., J. Photo physics of Aromatic Molecules, Wiley, London, UK (1970).
- [16] Kumar G.A. and Unnikrishnan N. V., energy transfer and optical gain studies of FDS: Rh B dye mixture investigated under cw laser excitation. *J. Photochemistry and Photobiology Chemistry*.144, 107-117 (2001).
- [17] El-Daly S. A., Photo physical properties: laser activity and energy transfer from 1, 4-bis [β - (2 benzothiazolyl) vinyl] benzene (BVB). *J. Photochem, Photobiol. A: Chem.* 124, 127-133(1999).
- [18] Deshpande A. V. and Namdas E. B., Efficient lasing action of Rhodamine 6G in Nafion membranes. *J. Chem. Phys. Letter*.263, 449-455 (1996).
- [19] Kumar S., Rao V.C. and Rastogi R. C. Excited-state dipole moments of some hydroxy coumarin dyes using an efficient solvato chromic method based on the solvent polarity parameter, *J. SpectrochimicaActa Part A*. 57, 41-47 (2001).
- [20] Pavlopoulos T.G., scaling of dye lasers with improved laser dyes. *J. Progress in Quantum electronics*.26, 193-224(2002).
- [21] Heldt J., J.R., Szezepanski J. and Diehl H.A., Gain and excited singlet and triplet state absorption spectra of some 9-acetoxy-10 (halogenoacetoxy) phenylanthracenes. *J. Appl. Phys. Chem. B* 46, 339-346(988).
- [22] Kawski A. and Rabek J. F. (Eds.), *Progress in Photochemistry and Photo physics* 5, 1-47 (1992).
- [23] Kawski A. And Naturforsch Z. Ground- and Excited-State Dipole Moments of 6-Propionyl-2-(dimethylamino) naphthalene Determined from Solvato chromic Shifts Luminescence Research Group, 54A, 379-381 (1999).

Laser Behavior of (E, E)-2, 5-Bis [2-(1-Methyl-1H-Pyrrole-2-Yl) Pyrazine (BMPP) Dye Hybridized with Cds Quantum Dots (Qds) in Sol-Gel Matrix and Various Hosts

- [24] Tipperudrappa J., Biradar D. S., Manohara S. R., Hanagodimath S. M. and Inamdar S. R., Solvent effects on the absorption and fluorescence spectra of some laser dyes: Estimation of ground and excited-state dipole moments, J. R. Mannekutla, Spectrochim. Acta, Part A 69, 991-997 (2008).
- [25] Reichardt C., Solvents and Solvent Effect in Organic Chemistry, third edition, Wiley-VCH, Verlag, GmbH and Co., KGaA, Weinheim, (2004).
- [26] Ravi M., Soujanya T., Samanta A., Radhakrishnan T. R. Excited-state dipole moments of some Coumarin dyes from a solvatochromic method using the solvent polarity parameter, E^N_T J. Chem. Soc. Faraday Trans. 91, 2739-2742 (1995).
- [27] Ebeid E. M. and Alhazmy S. M., Photophysical and Laser-Based Techniques Chemistry, Biology and Medicine, Book Surge Publisher, Charleston, SC USA (2006).
- [28] Pannipara M., Asiri A. M., Alamry K. A., Salem I. A. and El-Daly S. A. Structural and Photo physical Properties of (2E)-3-[4-(Dimethylamino) Phenyl]-1-(Naphthalen-1-yl) Prop-2-en-1-One (DPNP) in Different Media. J. Fluoresc. 25, 103– (2015)
- [29] Kabatc J., Osmialowski B. and Paczkowski J., Determination of the Ground and Excited State Dipole Moments of Some Hemicyanine Dyes. J. Spectrochim. Acta, Part A. 63 524-531 (2006).
- [30] Reichardt C., Solvatochromic Dyes as Solvent Polarity Indicators, J. Chem. Rev. 94, 2319–2358 (1994).
- [31] Kamlet M. J., Abboud J. L. M., Abraham M. H. and Taft R. W., Linear solvation energy relationships. 23. A comprehensive collection of the solvatochromic parameters, π^* , α . And β . And some methods for simplifying the generalized solvatochromic equation. J. Org. Chem. 48, 2877-2887 (1983).
- [32] Stamatovska V. and Dimova V., Solvent affects on electronic absorption spectra of some n-aryl substituted dodekanamides bull. Chem. Technol. Macedonia, 25, 9-16 (2006).

Citation: Mahmoud A. S. Sakr, Sayed A. Abdel Gawad, Samy A. El-Daly et al, "Laser Behavior of (E, E)-2, 5-Bis [2-(1-Methyl-1H-Pyrrole-2-Yl) Pyrazine (BMPP) Dye Hybridized with CdS Quantum Dots (QDs) in Sol-Gel Matrix and Various Hosts", *Research Journal of Nanoscience and Engineering*, 2019, 3(2), pp.1-12.

Copyright: © 2019 Mahmoud A. S. Sakr et al, This is an open-access article distributed under the terms of the Creative Commons Attribution License, which permits unrestricted use, distribution, and reproduction in any medium, provided the original author and source are credited.